Received: 27 January 2021 | Revised: 29 March 2021 | Accepted: 19 April 2021

DOI: 10.1111/ijac.13782

International Journal of Applied Ceramic TECHNOLOGY

RESEARCH ARTICLE

Characterization, in vitro bioactivity and biological studies of sol-gel-derived TiO_2 substituted 58S bioactive glass

Amirhossein Moghanian[1] | Saba Nasiripour[2] | Atiyyeh Koohfar[1] | Mohammad Sajjadnejad[3] | SeyedMohammad Hosseini[4] | Mohsen Taherkhani[5] | Zahra Miri[6] | Seyed Hesamedin Hosseini[1] | Mehrnaz Aminitabar[4] | Ali Rashvand[1]

[1]Department of Materials Engineering, Imam Khomeini International University, Qazvin, Iran

[2]School of Metallurgy and Materials Engineering, Faculty of Engineering, University of Tehran, Tehran, Iran

[3]Department of Materials Engineering, School of Engineering, Yasouj University, Yasouj, Iran

[4]Qazvin Science and Technology Park, Qazvin, Iran

[5]Department of Dermatology, Faculty of Medicine, Qazvin University of Medical Sciences, Qazvin, Iran

[6]Department of Materials Engineering, Isfahan University of Technology, Isfahan, Iran

Correspondence
Amirhossein Moghanian, Department of Materials Engineering, Imam Khomeini International University, Qazvin 34149-16818, Iran.
Email: Moghanian@eng.ikiu.ac.ir

Abstract

Bioactive glasses (BGs) have been used for bone formation and bone repair processes in recent years. This study investigated the titanium substitution effect on 58S BGs (Ti-BGs) $60SiO_2$-$(36 - X)CaO$-$4P_2O_5$-$XTiO_2$ ($X = 0$, 3, and 5 mol.%) prepared by the sol-gel technique, and the main goal was to find the optimum amount of titanium in Ti-BGs. Synthesized BGs, which were investigated after immersion in simulated body fluid (SBF), were tested by X-ray diffraction (XRD) analysis, Fourier transform infrared spectroscopy (FTIR), and scanning electron microscopy. Moreover alkaline phosphate (ALP) activity, 3-(4,5dimethylthiazol-2-yl)-2,5-diphenyltetrazolium bromide (MTT) assay, and antibacterial studies were employed to investigate the biological properties of Ti-BGs. According to the FTIR and XRD test results, hydroxyapatite (HA) formation on Ti-BGs surfaces was confirmed. Meanwhile, the presence of 5 mol.% compared to 3 mol.% increased the HA grain distribution and their size on the Ti-BGs surface. Additionally, MTT and ALP results confirmed that the optimal amount of titanium substitution in BG was 5 mol.%. Since 5 mol.% Ti incorporated BG (BG-5) had the highest biocompatibility level, antibacterial properties, maximum cell proliferation, and ALP activity among the synthesized Ti-BGs, it is presented as the best candidate for further in vivo investigations.

KEYWORDS

bioactive glass, biomedical applications, hydroxyapatite, sol-gel, TiO_2

1 | INTRODUCTION

According to previous reports, annually, many people's lives are endangered by bone defects.[1] For solving this problem, bone tissue engineering (BTE) has emerged as a powerful strategy based on recognizing the bone structure.[2] In other words, BTE is an approach that continues repairing bone defects by the patient's tissue to complete reconstruction.[3] Because bone is one of the most complex and dynamic connective tissues, it can regenerate different cells such as osteoblasts, osteoclasts, and bone cells through its combined function.[4] When a bone tissue hurts, it starts to regenerate itself, but it takes a long time or uses allograft isograft or xenograft can be risky or maybe cause an immune response. So, using an appropriate biomaterial can be a confident approach to accelerate the process of repairing.

Biomaterials are natural or artificial materials used for the healing or replacement of damaged tissues. The ideal biomaterial has some requirements, such as bioactivity, biodegradability, and cytocompatibility.[5,6] Bioactivity is one of the essential features of bioactive materials. In other words, the biomaterial is not the only kind of material that does not have any toxicity and harmful effects on the human body but also can form hydroxyapatite (HA) that is important.

When bioactive material is soaked in biological fluids such as simulated body fluid (SBF), the HA layer can be formed on their surfaces.[6–8] According to its biological passivity, it can be used inside the human body.[9] Biomaterials are produced by combining bioactive composites[10] and BGs to develop a hybrid system[11–13] and obtain dual-function implants as scaffolds for tissue engineering that bone-forming cells can regenerate bone in scaffolds and also personalized medicine.[14–16]

One of the first promising biomaterials that have been used in the mentioned process as a novel substitute for conventional metals and ceramics implants was bioactive glass (BG), which professor Hench invented in 1969.[17] BGs are a group of biomaterials that are generally based on amorphous silicate compounds and have been produced and used as bone grafts or fillers in bone repair and instauration.[7,18] According to the extreme development of BGs, various chemical compositions have been synthesized, such as 58S,[19] 68S, 77S,[20] with different synthesis methods such as conventional melt quench, flame synthesis, and microwave irradiation, as well as sol-gel.[21] The sol-gel process can be considered the easiest and the most efficient method at room temperature that increases purity and homogeneity.[22]

Bioactive glasses can be used for many orthopedic diseases treatment because of their properties such as bioactivity,[23] osteogenesis,[24] controllable biodegradability,[25] as well as antibacterial efficiency.[26–28] Actually, by making HA the prominent bone forming material on the BG surface, HA plays a vital role in healing teeth and bone tissues.[29] As a calcium-phosphate-based ceramic, HA ($Ca_{10}(PO_4)_6(OH)_2$) is the principal mineral part of the dental enamel and the hard tissue on the outside layer of human teeth and bone.[30–33] BG is the first synthetic solid to bond to natural bone [10,34,35] so in recent years, substituted BGs have become fascinated by scientists for their multifunctional capabilities due to replacing components. Many elements and combinations have been substituted in BGs for different applications, for example, suitable for dental and bone implants,[36] helpful for strengthening the mechanical properties,[37–39] exert a stimulatory effect on the osteoblast proliferation,[40] and release of proper ions that can act as antibacterial properties to the biomaterial.[41,42] Additionally, BGs have been investigated to design light-triggered and targeted drug delivery hybrids.[43–45]

Titanium, with the symbol of Ti, is an element with a biocompatibility property, which has been one reason for its use in BGs. Interestingly, when Ti gets oxidized, its properties like antibacterial and photocatalytic will be improved.[46] The antibacterial properties of BG have been previously noted.[47] Besides, BGs can lessen and prevent the risk of post-operative bacterial infections.[47] A bacterial infection prolonged the process of wound healing and leads to a surgical failure.[48] One of the leading causes of infections is methicillin-resistant *Staphylococcus aureus* (MRSA), which has long been known as a risk to human health due to its resistance to some antibiotics.[49,50]

There have been conflicting reports so far about the effect of Ti on Ti-incorporated silicon-based BG. Some researchers exhibited that Ti positively affected bioactivity, biocompatibility, cell proliferation, and cell viability.[51–53] Moreover some researchers have reported that the addition of Ti reduced cell viability, or in some cases, it was not noted that the presence of 5% Ti is optimal. Still, others did not observe biocompatibility.[54–56] Additionally, Rajendran et al. reported that[57] the addition of Ti above one mol.% reduced the HA forming ability.

Taken together, the specific object of this research was to consider the exact effect of different percentages of TiO_2 (in the range of 0–5 mol.%) on silicon-based sol-gel derived BGs-58S to investigate in vitro bioactivity, biocompatibility, alkaline phosphate (ALP) activity, 3-(4,5dimethylthiazol-2-yl)-2,5-diphenyltetrazolium bromide (MTT) assay, as well as quantitative antibacterial activity against MRSA bacteria properties. Furthermore, after immersion in SBF (a solution with an ionic concentration close to the human body plasma), the morphological and structural changes due to HA formation on BGs surfaces were perused by scanning electron microscopy (SEM), energy-dispersive X-ray spectroscopy (EDS), X-ray diffraction (XRD) analysis as well as Fourier transform infrared spectrum (FTIR) due to investigate the optimum amount of TiO_2 in synthesized Ti-BGs. Besides, considering the Ti effect on the ions release rate of Si, Ca, P, and Ti was carried out by the inductively coupled plasma-atomic emission spectroscopy (ICP-AES) test.

2 | MATERIAL AND METHODS

2.1 | Materials

In this study, to synthesize Ti substituted BG (Ti-BGs), three essential primary materials, including tetraethyl orthosilicate (TEOS), triethyl phosphate (TEP), and calcium nitrate tetrahydrate as the bases were required and to study the additive TiO_2 effect, tetraethyl orthotitanate (TEOT) was utilized. Besides, all of them were provided from Merck KGaA (Germany) with ≥99.0% purity, and for evaluating BG in vitro biological properties, SBF solution was used. The chemical compositions of the synthesized Ti-BGs are summarized in Table 1.

After synthesizing the powder, 9 MPa pressure was applied to discs with 1 cm diameter and 0.3 g weight by a hydraulic press. Afterward, discs were soaked in 15 ml SBF solution prepared according to Kokubo's protocol[58] for 1, 3, 7, 14, and 21 days, then removed from the SBF solution dried to study in vitro evaluations.

TABLE 1 All composition of synthesized Ti substituted bioactive glass (BG, in mol.%)

Bioactive glass	Label	SiO_2	CaO	P_2O_5	TiO_2
58S-0%TiO_2	BG-0	60	36	4	0
58S-3%TiO_2	BG-3	60	33	4	3
58S-5%TiO_2	BG-5	60	31	4	5

2.2 | BGs synthesis

Tetraethyl orthotitanate with two different concentrations of (3 and 5 mol.%) and mentioned materials were synthesized through the sol-gel method to obtain the quaternary Ti-BGs. For preparing a homogeneous solution (Sol), at first, a specific amount of distilled water and 0.1 N HNO_3 were mixed in a beaker and stirred on a magnetic stirrer for 30 min, followed by TEOS and TEP were added to the solution separately. After adding each of them, the solution was stirred for 45 min, and finally, after adding TEOT, the solution was stirred for 1 h. After the end of gel synthesis, to obtain a dry powder, the solution was first incubated for 3 days at room temperature; secondly, it was heated by oven at 75°C for 3 days; finally, it was heated in a furnace at 650°C for 3 h. Moreover it should be noticed that during the exiting of gases and evaporation of water, the beaker surface should be covered with thin plastic to prevent any contamination from entering, and the presence of a few small cavities was enough on thin plastic to release gas and vapor.

2.3 | Characterization of BGS

2.3.1 | X-ray diffraction analysis

To investigate HA formation on BGs surfaces, the surfaces of the specimens were exposed to XRD after soaking in SBF solution for 1, 7, and 14 days with X-ray source (Cu-Kα radiation) at 40 kV and in a 2θ range of 20°–40°.

2.3.2 | Fourier transform infrared spectroscopy analysis

Fourier transform infrared spectrum spectroscopy (Nicolet, NEXUS 670) was applied to examine HA phase formation on the specimen surface before and after soaking in the SBF solution by analyzing functional groups shifts in the 8 cm^{-1} resolution 400–4000 cm^{-1} wavelength.

2.3.3 | Scanning electron microscopy

After immersion in the SBF solution, SEM (MIRA3 TESCAN, Czech) was used to observe the BG disks' surface morphology to evaluate HA formation and its growth over immersion time in the SBF solution.

2.3.4 | Inductively coupled plasma-atomic emission spectroscopy

Specimens kept in SBF solutions were removed after 12 h and 1, 3, 7, 14, and 21 days and solutions were analyzed by ICP-AES for Ca, Si, P, and Ti ions investigation. Besides, pH change with immersion time in the SBF solution was measured by a pH meter (Corning pH meter 340) at each step.

2.4 | Biological evaluation

2.4.1 | MTT and ALP activity assays

The 3-[4,5-dimethylthiazol-2yl]-2,5-diphenyl-2H tetrazolium bromide (MTT) assay was performed to appraise proliferation of the MC3T3-E1 cells after in contact with different synthesized Ti-BG. In the MTT test, living cells be able to degrade the tetrazolium salt and create formazan. Moreover in this study, the measuring ALP enzyme investigated the osteoblastic activity of the MC3T3-E1 cells. Based on the manufacturer's recommendations (BioCat), the MC3T3-E1 cells with a density of 1×10^4 cells cm^{-2} plated and cultured in 24-well plates on specimens under a humidified atmosphere of 95% air and 5% carbon dioxide at 37°C for 1, 3, and 7 days. Enzyme activity was assessed at 410 nm for the amount of p-nitrophenyl disodium salt (pNPP, 16 mmol L^{-1}; Sigma-Aldrich Company) liberated.[59–61]

2.4.2 | Antibacterial studies

Methicillin-resistant *S. aureus* was cultured in liquid lysogeny broth (LB) medium at 37°C. Before tests, bacteria were diluted approximately to 0.5×10^8 to 2×10^8 ml^{-1}.[44,59] To investigate the effect of Ti on antibacterial activities in Ti-BGs, 0.9 ml LB medium was added into three 1.5 ml Eppendorf tubes containing 10 mg BG-0 (control specimen), BG-3, and BG-5 particles followed by stirring for 1 min. Then 0.1 ml bacterial suspension was added into each Eppendorf tube, and the solutions were cultured at 37°C for 1 h. A sequential dilution was performed in the next step, then by incubating LB-agar plates in the darkness and the temperature of 37°C, 100 μl suspensions put on them.[44] Ultimately through final colony-forming units per milliliter, the survivor bacteria percentage was determined (CFU ml^{-1}).[47,62-64]

$$\text{Bactericidal fraction} = 1 - \left(\frac{\text{number of survived bacteria}}{\text{number of total bacteria}}\right).$$

3 | RESULT AND DISCUSSION

3.1 | X-ray diffraction analysis

Figure 1 displays the XRD patterns of BG-0, BG-3, and BG-5, respectively, before and after soaking in the SBF solution for 1, 7, and 14 days. In the present investigation, the XRD results, Figure 1A–C, showed no HA crystalline before immersion in the SBF solution because of the amorphous structure. However, after soaking in the SBF solution, two peaks at 2 thetas equal to 25.8° (assign to (200) plane) and 31.8° (set to (211) plane) affirmed the formation of crystalline HA on the BG surface according to the standard the joint committee on powder diffraction standards cards (no. 09-432).[65] Besides, through the time to 14 days, HA peaks were pronounced due to increasing aggregation and HA crystalline growth. XRD patterns of BG-5 exhibited a similar trend as BG-0 and BG-3 with higher intensity.

Additionally, the results showed that by increasing the Ti percentage, the HA formed on the Ti-BG surface-enhanced. It was reported that up to 14 days, the peak intensity of BG-0 and BG-5 increased.[52] Although Ti retarded the HA formation in the first time of immersion and its effect diminished, Ti increased the HA formed overtime of soaking in the SBF solution. Similarly, this effect of Ti on HA formation was observed in our XRD results.

3.2 | FTIR analysis

As shown in Figure 2A, the amount of phosphate and carbonate in the control specimen increased until the 14th day

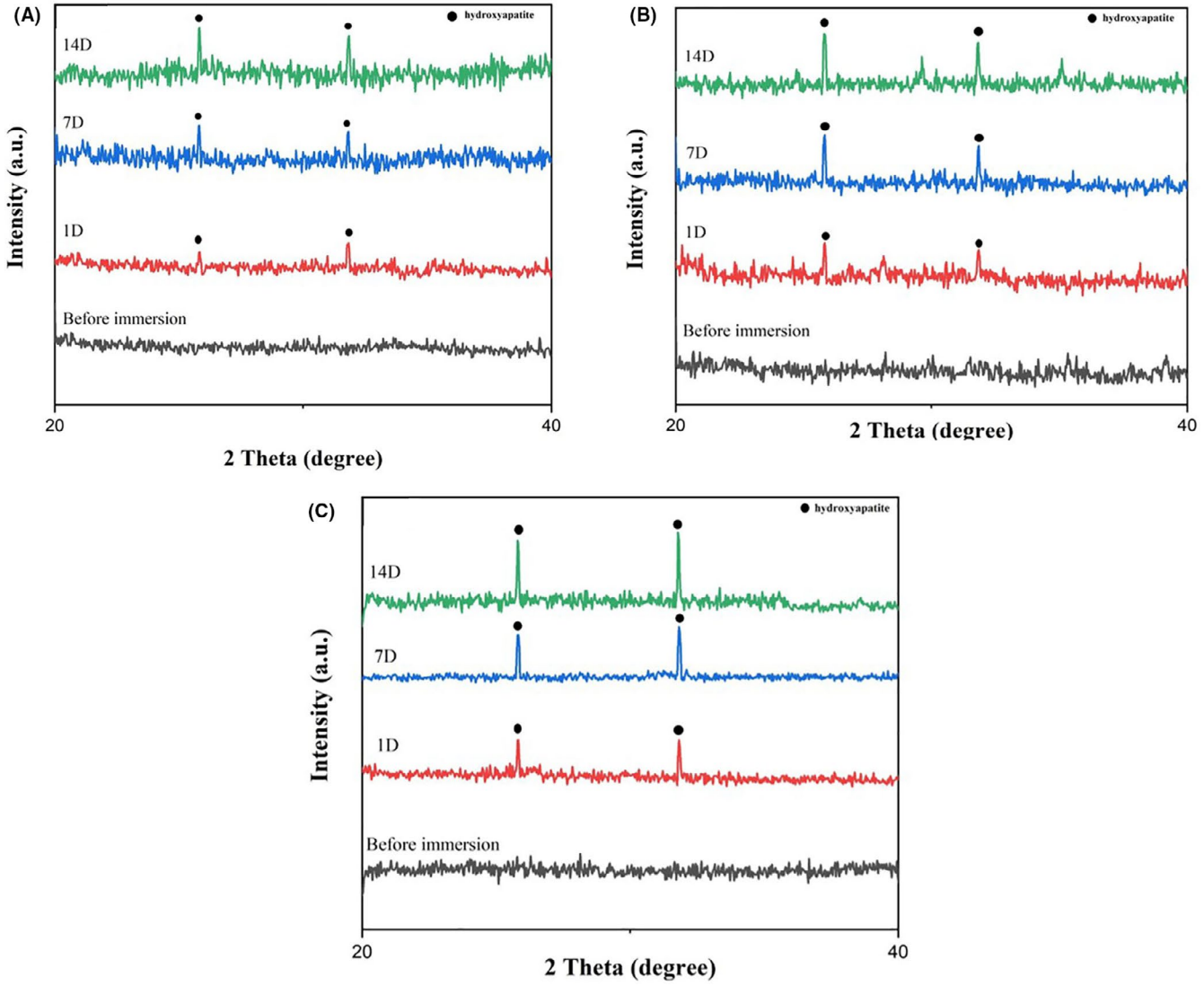

FIGURE 1 X-ray diffraction patterns of (A) bioactive glass (BG)-0, (B) BG-3, and (C) BG-5 before and after soaking in simulated body fluid solution for 1, 7, and 14 days

and stabilized. Therefore, according to the diagram, it can be concluded that carbonate and phosphate (HA) were formed. According to Figure 2B, it can be mentioned that in the presence of 3 mol.% TiO_2, the amount and rate of carbonate and phosphate formation have increased in comparison with its absence (Figure 2). On the seventh day, a significant decrease was observed, which resolved in the coming days, and the amount of HA increased.

By adding 5 mol.% to the BG (Figure 2C), on the 14th day, the amount of HA formation had a sudden increase, which indicated the appearance and rise of HA. The FTIR analysis observed bonds[41,44,46,58,62] are shown in Table 2. HA maturation is the gradual conversion of non-apatite domains to weak crystallization followed by HA crystallization.[33] While, Bargavi et al.[66] reports did not mention the presence of a bond between Si and Ti, Danewalia et al.[67] reports confirmed these bonds' formation. Our results were in good agreement with Danewalia et al.[67] findings, which showed that Ti is generally present in silicate and borate glasses in the Ti^{4+} state (TiO_2), and the IR bands became sharper at higher Ti content, which showed a more orderly local structure of the glasses. Similarly, as the other authors reported,[67-74] it was confirmed from FTIR results that Ti substituted caused the Si–O–Ti bond at 930 cm^{-1}, which confirmed the interaction between Ti and BGs.

3.3 | Surface morphology

The SEM images in Figure 3 demonstrate the BG surface before soaking in the SBF solution and display the immersion results of BG-0, BG-3, and BG-5 in SBF solution for 1, 7, and 14 days, respectively. Meanwhile, Figure 4 exhibits the EDS analysis of Ti-BGs after 14 days of immersion in the SBF solution. Moreover the transmission electron microscopy (TEM) image of BG-5 after 14 days immersion in the SBF solution is shown in Figure 5. According to the SEM images, the first spherical globules of HA have appeared in the first 24 h of immersion. Additionally, by increasing the

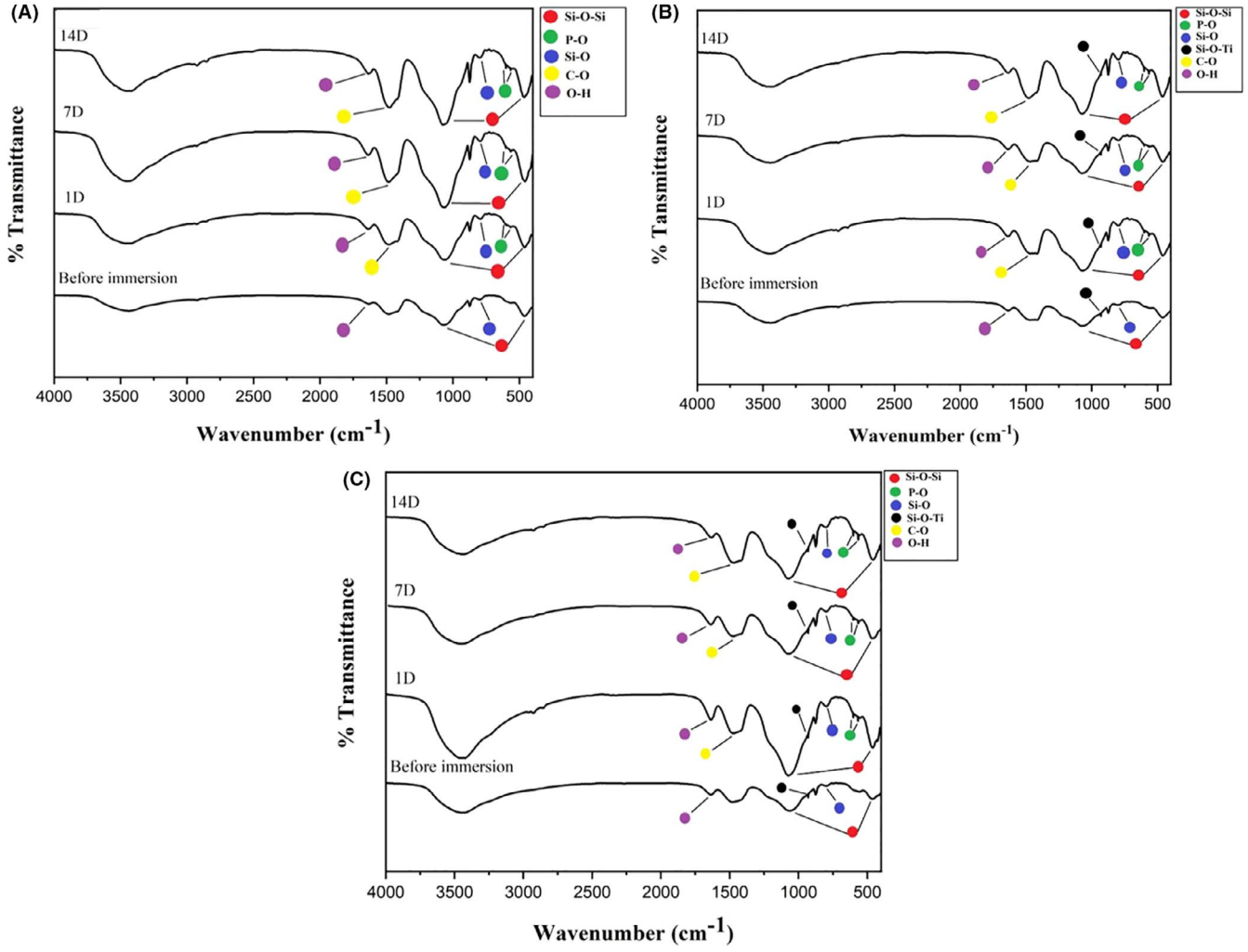

FIGURE 2 Fourier transform infrared spectroscopy spectroscopy of (A) bioactive glass (BG)-0, (B) BG-3, and (C) BG-5 before and after immersion for 1, 7, and 14 days

Wavenumber (cm^{-1})	Assignment
420	Si–O–Si bending vibration
570	Asymmetric vibration of PO_4^{3-}
800	Si–O–Si symmetric stretching vibration
930	Si–O–Ti bond
1070	Si–O–Si asymmetric stretching vibration
1455	C–O stretching in carbonate groups
1670	Stretching of OH group

TABLE 2 Assignment of Fourier transform infrared spectroscopy per wavenumber

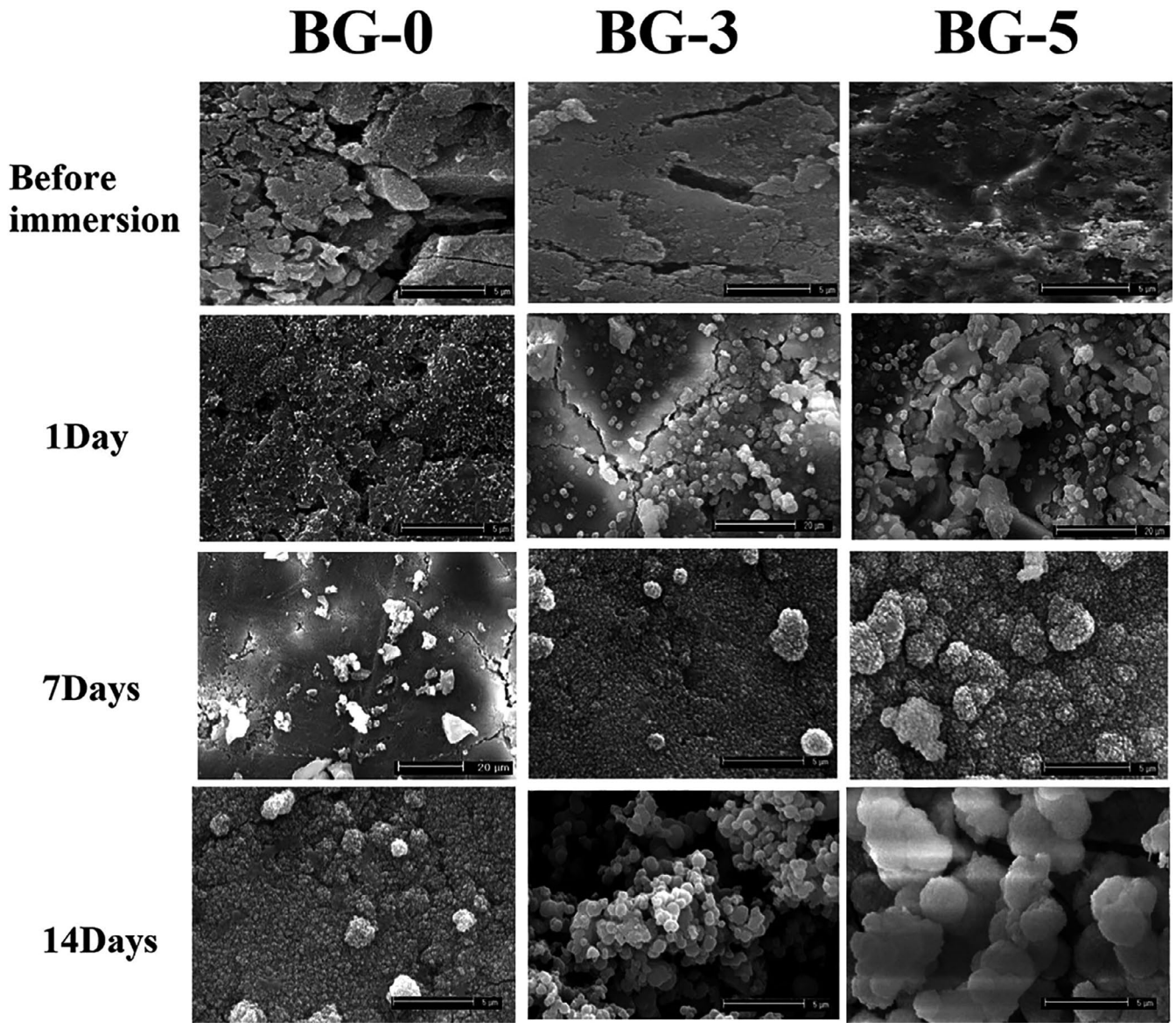

FIGURE 3 Scanning electron microscopy pictures of Ti-BGs specimens before and after immersion in the simulated body fluid solution for 1, 7, and 14 days. Ti-BG, Ti substituted bioactive glass

immersion time, the amount of HA on the BG surface was enhanced. Additionally, the increase in the nucleation rate and aggregation of HA on the surface was quite noticeable.

The process was like that; first, the HA globules have nucleated on the BG surface, and afterward, by increasing time up to 14 days, they grew and gathered together to agglomerate. On the first day, it was evident that HA globules started to agglomerate and made greater HA globules with a spherical shape. Eventually, they were stabilized in 14 days, and HA entirely covered the BG surface. Moreover

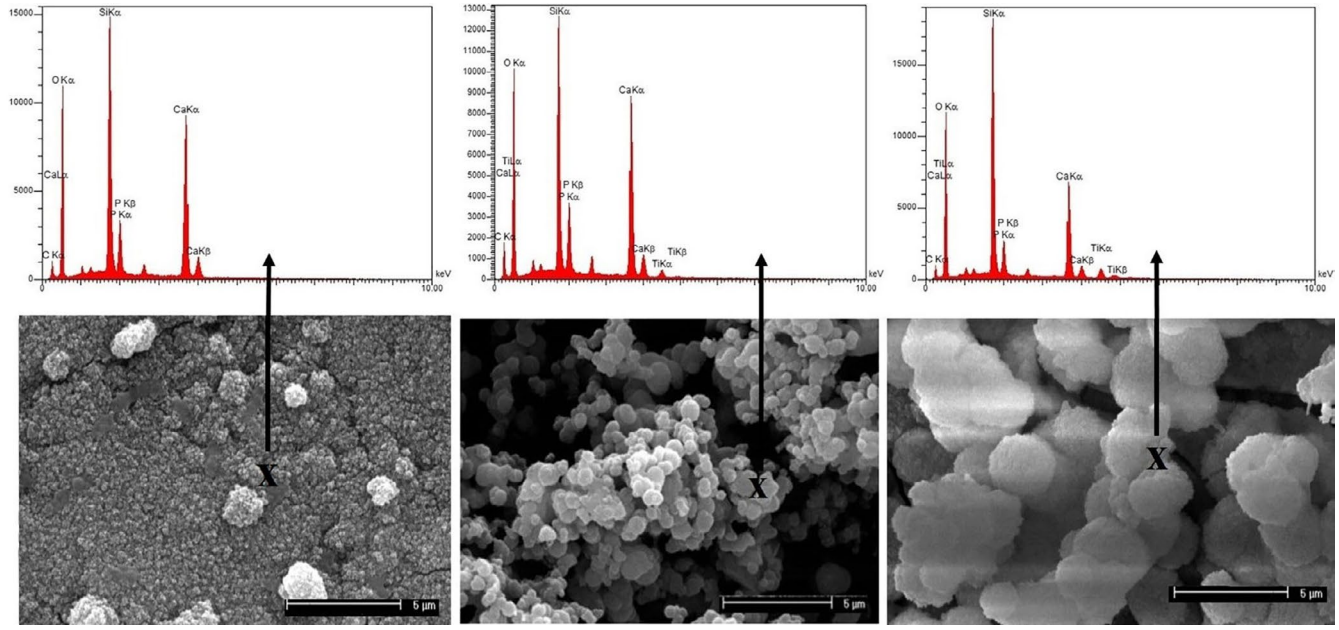

FIGURE 4 Energy-dispersive X-ray spectroscopy analysis of Ti-BGs after 14 days immersion in the simulated body fluid solution. Ti-BG, Ti substituted bioactive glass

FIGURE 5 TEM image of bioactive glass (BG)-5 after immersion in the simulated body fluid solution for 14 days

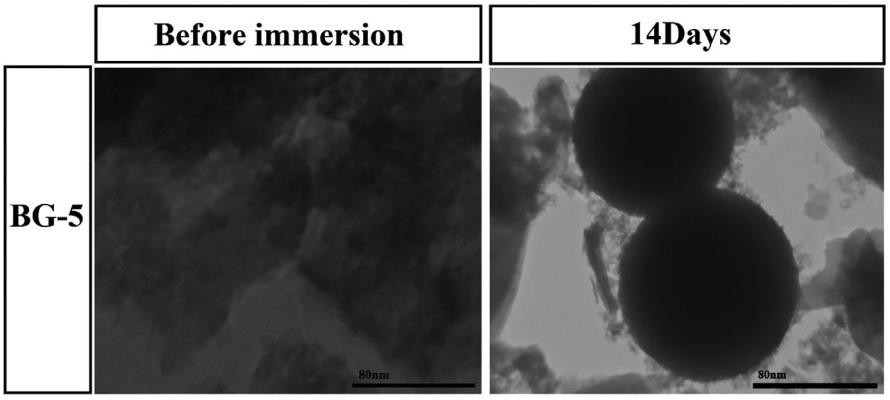

increasing the percentage of TiO_2 (3 and 5 mol.%) played a significant role in growing the amount and size of HA grain on the surface. Furthermore, after 14 days of immersion of BG-5 in the SBF solution, the TEM image confirmed HA globules' formation with a diameter of more than 80 nm, and also, the EDS image supported the Ca/p ratio close to 1.67.

Meanwhile, it was reported that with an increase in the percentage of TiO_2 more than 5 mol.%, the formation of HA decreased.[52] Additionally, Ben-Arfa et al.[51] reported that all BGs with substitution of Ti displayed a quick biomineralization rate due to HA formation on the BG surface after 1 h of soaking in the SBF solution. Therefore, they showed a high bioactivity rate, and it accelerated by increasing time up to 7 days. In the previous study,[57] it was investigated that Ti-substituted BG with 1 mol.% TiO_2 exhibited better bioactivity and biocompatibility compares to BGs with substitution of 0, 2, and 3 mol.% TiO_2.

3.4 | ICP analysis

Based on ICP results, the rate change of Ca, P, Si, and Ti ions function with time on BGs are illustrated in Figure 6. To determine the Ca, P, Si, and Ti ions release trend, the BGs were immersed in the SBF solution for 1, 3, 7, and 14 days and the release rate was measured. According to the results, Si and Ca exhibited a downward trend after a sudden increase in 3 days. The ion release trend of the p element was entirely downward with the various rate at different times due to HA formation. Furthermore, the ion release rate of Ti was dependent on the Ti amount in BGs and differed. By increasing the Ti amount in BGs, the Ti ions release decreased. Actually, by substituting Ti to Ca, the BG network became compact due to fewer ion radius of Ti (68 ppm) than Ca (100 ppm). Furthermore, this substitution led to a decrease in network disorder and BG solubility. In other words, BG-0 and BG-5 displayed the most and the least ions releasing in the SBF solution overtime,

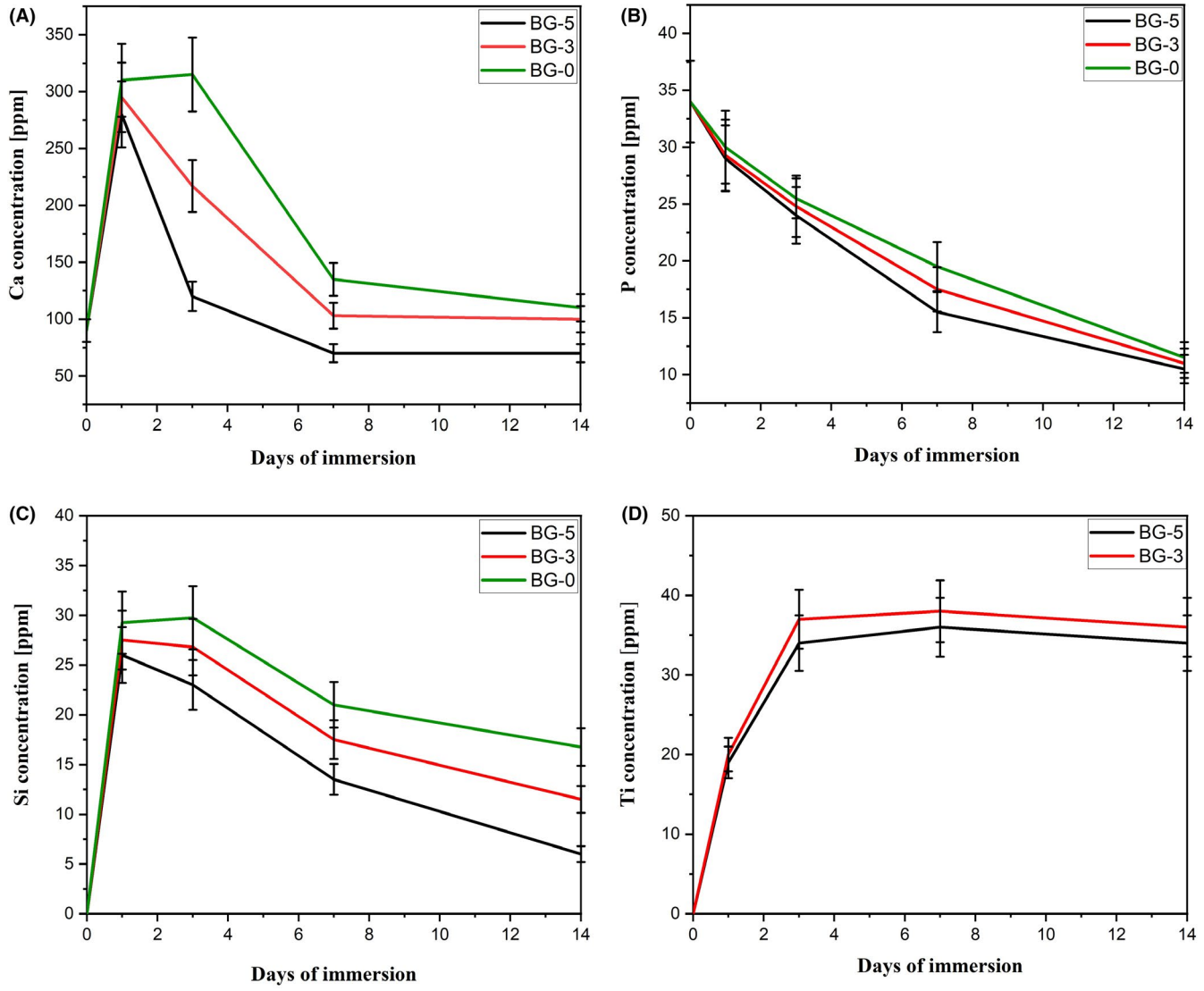

FIGURE 6 Inductively coupled plasma-atomic emission spectroscopy test results of Ca (A), P (B), Si (C), and Ti (D) elements on Ti-BGs. Ti-BG, Ti substituted bioactive glass

respectively. Besides, in Figure 6D, the Ti concentration rate in the SBF solution increased in the first 3 days of immersion, and followed by, the Ti ions release slightly decreased. Taken together, an increase in Ti amount in BGs led to a decrease in ions releasing concentration of Ca, P, Si, and Ti in all incubation times. In previous research, Mohammadi et al.[55] reported that in sodium-free calcium phosphate-based glasses substituted with 0, 3, 5, 7, and 10 mol.% TiO_2, increasing Ti percentage in bioglass had a diverse effect on ion releasing amount, and the concentration of P, Ca, Si, and Ti decreased overtime. Moreover Abou Neel et al.[70] stated that when 0, 1, 3, and 5 mol.% Ti dioxide substituted with NaO_2 in phosphate-based glasses, by increasing Ti amount in the glass composition, the ICP test results exhibited a reduction rate in ions releasing of P, Si, Ca. According to previous studies, our results were in good agreement with them in the Ti ion release rate, and they display the same trend with different compositions.

3.5 | In vitro biological evaluation

3.5.1 | MTT assay

The MTT cytotoxicity assay results of BG-0, BG-3, and BG-5 after incubation for 1, 7, and 14 days are exhibited in Figure 7. As it was apparent after the first day of incubation, BG-5 demonstrated an increase in MTT activity of MC3T3.E1 cells ($^*p < 0.05$). Additionally, by increasing the TiO_2 percentage, the cell viability increased, and cytotoxicity decreased in incubation times. After 7 days of incubation, the BG-5 showed the highest mean absorbance ($^{**}p < 0.01$). On the other hand, on the 14th day of culture, it had the most elevated cell proliferation than others ($^{***}p < 0.001$). Accordingly, BG-5 can be contemplated as the optimal specimen. Previously Heidari et al.[52] reported that the BG-ceramic with 5 mol.% TiO_2 was the optimum one compared to BGs with a high and low TiO_2

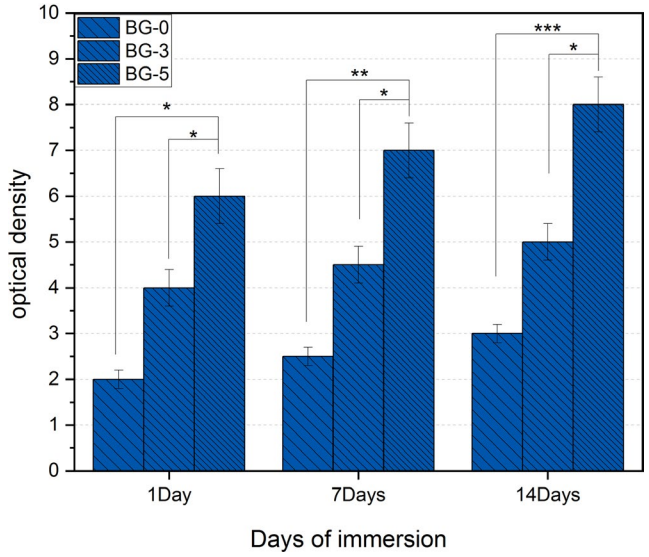

FIGURE 7 In vitro biocompatibility of bioactive glass (BG)-0, BG-3, and BG-5 by 3-(4, 5dimethylthiazol-2-yl)-2, 5-diphenyltetrazolium bromide assay in osteoblast cell line (*$p < 0.05$, **$p < 0.01$, and ***$p < 0.001$)

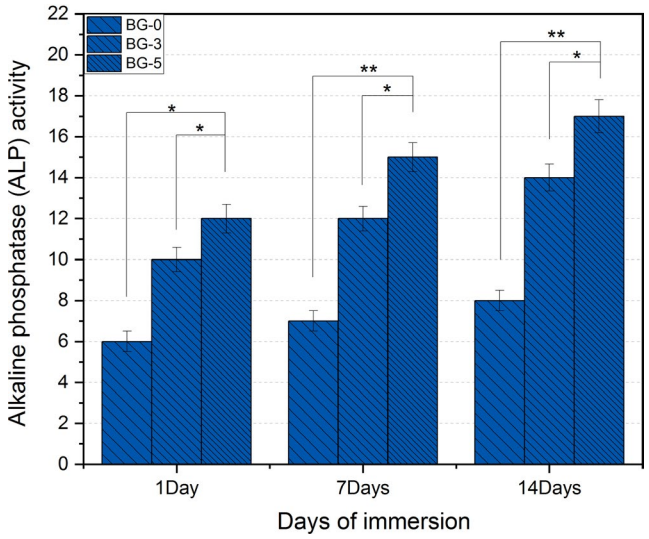

FIGURE 8 Alkaline phosphate activities of an osteoblast-like cell line (MC3T3E1) cultured on bioactive glass (BG)-0, BG-3, and BG-5 for 1, 7, and 14 days of immersion. (*$p < 0.05$ and **$p < 0.01$)

percentage. Because of an increase in TiO_2 percentage, more than 5 mol.%, cell viability, and cell proliferation descended. Additionally, in 2015 Rajendran et al.[57] reported that Ti-substituted BG with 1 mol.% TiO_2 was the optimum composition compared to BGs with substitution of 0, 2, and 3 mol.% TiO_2 because of higher cell viability and more dissolubility that caused an appropriate environment for cell proliferation and attachment. Therefore, with MTT results, it could be understood that BG-5 demonstrated the highest cell proliferation and mean absorbance in comparison to BG-0 and BG-3.

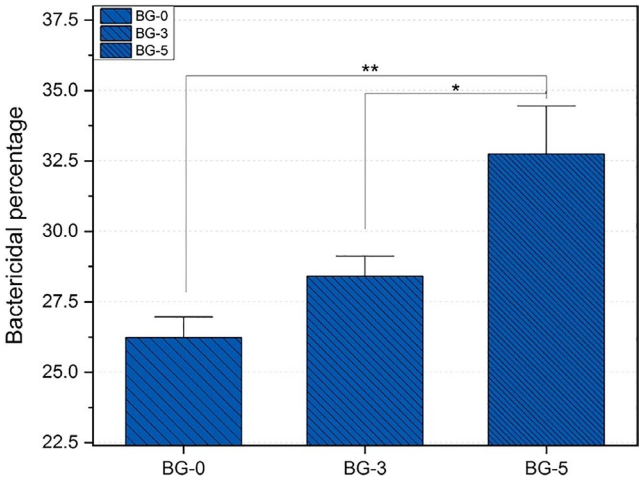

FIGURE 9 Quantitave bactericidal percentage of antibacterial activity of bioactive glass (BG)-0, BG-3, and BG-5 (*$p < 0.05$ and **$p < 0.01$)

3.5.2 | ALP activity

The changing procedure of ALP activity of osteoblast-like cell line MC3T3-EL cultured on BG-0, BG-3, and BG-5 for different times are demonstrated in Figure 8. On the first day of culture, BG-5 showed the highest ALP activity than BG-0 (*$p < 0.05$). The ALP activity ascended by increasing the TiO_2 percentage up to 5 mol.% in all incubation times. Additionally, by increasing time up to 14 days, ALP activity rose, and BG-5 showed the highest ALP activity compared to BG-0 (**$p < 0.01$). According to previous studies, Haidari et al.[52] investigated the influence of substitution of Ti on BG. It was reported that Ti substitution on BGs notably showed higher ALP activity than other BGs in all incubation times. Additionally, BG-5 exhibited the highest cell viability and ALP activity. The addition of 5 mol.% TiO_2 to BG is the optimal amount for addition. Likewise, Mohammadi et al.[55] reported that the highest ALP activity is related to the BG substituted by 3–5 mol.% TiO_2.

3.5.3 | Antibacterial analysis

For a wide selection of bacteria, it was proved that BGs have strong antibacterial effects, and with BGs concentration, the antibacterial properties increase.[75,76] The antibacterial assay was done on BG-0, BG-3, and BG-5. The results were displayed in Figure 9. According to that, TiO_2, as a powerful antibacterial substance, exhibited its effect on Ti-substituted BG. As it was evident, Ti-BGs showed high antibacterial efficiency in comparison with BG-0.

Furthermore, by increasing TiO_2 percentage, the antibacterial efficiency increased against MRSA at 0.01 g ml^{-1} concentration compared to BG-0. Additionally, BG-5 exhibited a significant increase in antibacterial efficiency compared to BG-0

(***$p < 0.01$). According to previous researches, Rajendran et al.[57] reported that by increasing TiO_2 percentage, the antibacterial activity enhanced, and Ti-substituted BG by 3 mol.% TiO_2 showed the highest inhibition zone in comparison to BGs with substitution of 0, 1, and 2 mol.% TiO_2. By increasing incubation time, antibacterial efficiency increased. Additionally, it was reported that Ti-substituted BGs showed high antibacterial activity against *E. coli* because of inducing a considerable amount of hydroxyl radicals against gram-negative bacteria.[57] The definite mechanism responsible for the antibacterial efficiency of BGs is yet unknown, but there were some possible reasons. One of them was releasing the alkaline earth ions that led to an increase in pH values, and the other one was the presence of calcium and phosphate ions that exert a toxic effect on bacteria.[77] Hence, increasing the percentage of TiO_2 more than 5 mol.% led to decreasing the biological properties.[52,55] So, BG-5 demonstrated the highest antibacterial efficiency in comparison to BG-0 and BG-3.

4 | CONCLUSION

As a result, the BG-58S with the formula $60SiO_2$-$(36 - X)$ CaO-$4P_2O_5$-$XTiO_2$ (X = 0, 3, and 5 mol.%) synthesized by the sol-gel method, and the influence of Ti-substituted BG was investigated. The main object of this investigation was to understand the optimal percentage of Ti (0, 3, and 5 mol.%) in Ti-BGs. The results include the following items:

1. In XRD patterns, two peaks at 2 thetas equal to 25.8° (assign to (200) plane) and 31.8° (assign to (211) plane) affirmed the formation of HA after immersion in the SBF solution. In the first time of soaking, Ti retarded the HA formation, but it had no effect in retarding, and the intensity of the characteristic peaks increased for a long time. Also, by increasing TiO_2 percentage up to 5 mol.%, peaks intensity increased. In other words, BG-5 exhibited a similar trend as BG-0 and BG-3 with higher intensity.
2. FTIR results confirmed HA formation and showed Si, O, P, H, and Ti bonds. The presence of Ti in the BG-58S facilitated the formation of HA. Furthermore, the company of 5 mol.% can be considered the optimal presence of TiO_2 in this BG.
3. In SEM images, the formation of HA is significant after 1 day of immersion in the SBF solution. Additionally, by increasing time up to 14 days, the aggregation of HA on the BG surface ascended. Furthermore, by increasing the percentage of TiO_2 up to 5 mol.%, the amount of HA increased on the BG surface. Additionally, the EDS analysis confirmed the formation of HA on the BG surface. Furthermore, the TEM image of BG-5 after 14 days of immersion in the SBF solution confirmed the HA formation on the BG surface.
4. The ICP-AES was carried out to measure Ti's addition effect on the ion release rate of Ca, Si, P, and Ti. The results indicated that increasing the Ti percentage had the opposite effect on the release of ions.
5. According to ALP and MTT assays results, BG-5 exhibited the highest cell viability and cell proliferation and no cytotoxicity compared with BG-0 and BG-3. Additionally, by increasing the time and percentage of TiO_2, up to 21 days and 5 mol.%, the bioactivity and antibacterial efficiency were enhanced. Hence, the BG-5 can be considered as the optimal specimen in comparison to BG-0 and BG-3.

ORCID

Amirhossein Moghanian https://orcid.org/0000-0002-7978-5968

REFERENCES

1. d'Aquino R, De Rosa A, Lanza V, Tirino V, Laino L, Graziano A, et al. Human mandible bone defect repair by the grafting of dental pulp stem/progenitor cells and collagen sponge biocomplexes. Eur Cells Mater. 2009;18(7):75–83.
2. Nerem RM. Tissue engineering: confronting the transplantation crisis. Proc Inst Mech Eng H J Eng Med. 2000;214(1):95–9.
3. Pina S, Oliveira JM, Reis RL. Natural-based nanocomposites for bone tissue engineering and regenerative medicine: a review. Adv Mater. 2015;27(7):1143–69.
4. Saatchi A, Arani AR, Moghanian A, Mozafari M. Synthesis and characterization of electrospun cerium-doped bioactive glass/chitosan/polyethylene oxide composite scaffolds for tissue engineering applications. Ceram Int. 2021;47(1):260–71. https://www.sciencedirect.com/science/article/pii/S0272884220325116
5. Siemionow M, Bozkurt M, Zor F. Regeneration and repair of peripheral nerves with different biomaterials. Microsurgery. 2010;30(7):574–88.
6. Perardi A, Cerrruti M, Morterra C. Carbonate formation on sol-gel bioactive glass 58S and on Bioglass® 45S5. Stud Surf Sci Catal. 2005;155:461–9.
7. Moghanian A, Tajer M, Zohourfazeli M, Miri Z, Saghafi YM. Sol-gel derived silicate-based bioactive glass: studies of synergetic effect of zirconium and magnesium on structural and biological characteristics. J Non Cryst Solids. 2021;554:120613. https://www.sciencedirect.com/science/article/abs/pii/S0022309320307237?dgcid=rss_sd_all
8. Moghanian A, Zohourfazeli M, Tajer M, Miri Z, Hosseini S, Rashvand A. Preparation, characterization and in vitro biological response of simultaneous co-substitution of Zr^{+4}/Sr^{+2} 58S bioactive glass powder. Ceram Int. 2020. https://doi.org/10.1016/j.ceramint.2020.11.139
9. Kasemo B. Biocompatibility of titanium implants: surface science aspects. J Prosthet Dent. 1983;49(6):832–7.
10. Pazhouheshgar A, Moghanian A, Sadough Vanini S. The extended finite element method numerical and experimental analysis of mechanical behavior of polysulfone/58s bioactive glass synthesized through solvent casting method. Modares Mech Eng. 2020;20(8):2061–73.

11. Salandari-Jolge N, Ensafi A, Rezaei B. A novel three-dimensional network of $CuCr_2O_4$/CuO nanofibers for voltammetric determination of anticancer drug methotrexate. Anal Bioanal Chem. 2020;412(11):2443–53.
12. Matter MT, Furer LA, Starsich F, Fortunato G, Pratsinis SE, Herrmann, IK, et al. Engineering the bioactivity of flame-made ceria and ceria/bioglass hybrid nanoparticles. J ACS Appl Mater Inter. 2018;11(3):2830–9.
13. Vukajlovic D, Parker J, Bretcanu O, Novakovic K. Chitosan based polymer/bioglass composites for tissue engineering applications. J Mater Sci Eng C. 2019;96:955–67.
14. Khorsandi D, Moghanian A, Nazari R, Arabzadeh G, Borhani S. Personalized medicine: regulation of genes in human skin ageing. J Allergy Ther. 2016;7(245):1–9. https://www.researchgate.net/profile/Ghazaleh-Arabzadeh/publication/315808906_Personalized_Medicine_Regulation_of_Genes_in_Human_Skin_Ageing/links/58e756694585152528de6074/Personalized-Medicine-Regulation-of-Genes-in-Human-Skin-Ageing.pdf
15. Gao C, Liu T, Shuai C, Peng S. Enhancement mechanisms of graphene in nano-58S bioactive glass scaffold: mechanical and biological performance. Sci Rep. 2014;4(1):1–10.
16. Arrigoni C, Gilardi M, Bersini S, Candrian C, Moretti M. Bioprinting and organ-on-chip applications towards personalized medicine for bone diseases. Stem Cell Rev Rep. 2017;13(3):407–17.
17. Hench LL, Jones JR. Bioactive glasses: frontiers and challenges. Front Bioeng Biotechnol. 2015;3:194.
18. Moghanian A, Firoozi S, Tahriri M. Characterization, in vitro bioactivity and biological studies of sol-gel synthesized SrO substituted 58S bioactive glass. Ceram Int. 2017;43(17):14880–90.
19. Moghanian A, Koohfar A, Hosseini S, Hosseini S, Ghorbanoghli A, Sajjadnejad M, et al. Synthesis, characterization and in vitro biological properties of simultaneous co-substituted Ti+4/Li+158s bioactive glass. J Non Cryst Solids. 2021;561:120740. https://www.sciencedirect.com/science/article/abs/pii/S0022309321000995
20. Cerruti M, Magnacca G, Bolis V, Morterra C. Characterization of sol-gel bioglasses with the use of simple model systems: a surface-chemistry approach. J Mater Chem. 2003;13(6):1279–86.
21. Li N, Jie Q, Zhu S, Wang R. Preparation and characterization of macroporous sol-gel bioglass. Ceram Int. 2005;31(5):641–6.
22. Dislich H. Sol-gel 1984→2004 (?). J Non Cryst Solids. 1985;73(1):599–612.
23. Ma J, Chen C, Wang D, Meng X, Shi J. Influence of the sintering temperature on the structural feature and bioactivity of sol-gel derived SiO_2–CaO–P_2O_5 bioglass. Ceram Int. 2010;36(6):1911–6.
24. Moura J, Teixeira L, Ravagnani C, Peitl O, Zanotto ED, Beloti M, et al. In vitro osteogenesis on a highly bioactive glass-ceramic (Biosilicate®). J Biomed Mater Res. 2007;82(3):545–57.
25. Yao A, Wang D, Fu Q, Huang W, Rahaman M. Preparation of bioactive glasses with controllable degradation behavior and their bioactive characterization. Chin Sci Bull. 2007;52(2):272–6.
26. Coraça-Huber DC, Fille M, Hausdorfer J, Putzer D, Nogler M. Efficacy of antibacterial bioactive glass S53P4 against *S. aureus* biofilms grown on titanium discs in vitro. J Orthop Res. 2014;32(1):175–7.
27. Moghanian A, Zohourfazeli M. Comparative study on in vitro, physico-chemical and antibacterial properties of 58S and 68S bioactive glasses synthesized by sol-gel method. Adv Process Mater. 2020;17–30. https://www.sid.ir/en/Journal/ViewPaper.aspx?ID=716955
28. Moghanian A, Zohour FM. Investigation the In vitro and bactericidal properties of magnesium and copper containing bioactive glasses. J Adv Mater Technol. 2020;9(2):19–33.
29. Kokubo T. Formation of biologically active bone-like apatite on metals and polymers by a biomimetic process. Thermochemica Acta. 1996;280:479–90.
30. Nobre C, Pütz N, Hannig M. Adhesion of hydroxyapatite nanoparticles to dental materials under oral conditions. Scanning. 2020;2020:1–12.
31. Tahriri M, Del Monico M, Moghanian A, Yaraki M, Torres R, Yadegari A, et al. Graphene and its derivatives: opportunities and challenges in dentistry. Mater Sci Eng C. 2019;102:171–85. https://www.sciencedirect.com/science/article/abs/pii/S0928493119302097
32. Lee S-M, Yoo K-H, Yoon S-Y, Kim I-R, Park B-S, Son W-S, et al. Enamel anti-demineralization effect of orthodontic adhesive containing bioactive glass and graphene oxide: an in-vitro study. Materials. 2018;11(9):1728.
33. Aminitabar M, Moghan A, Elsa M. Synthesis and in vitro characterization of a gel-derived SiO_2-CaO-P_2O_5-SrO-Li_2O bioactive glass. Int J Chem Mol Eng. 2019;13(6):296–307.
34. Pazhouheshgar A, Vanini S, Moghanian A. The experimental and numerical study of fracture behavior of 58S bioactive glass/polysulfone composite using the extended finite elements method. Mater Res Express. 2019;6(9):095208.1–12. https://iopscience.iop.org/article/10.1088/2053-1591/ab3495/meta
35. Zohourfazeli M, Mahdi Tajer MH, Moghanian A. Comprehensive investigation on multifunctional properties of zirconium and silver co-substituted 58S bioactive glass. Ceram Int. 2020;47(2):2499–507.
36. Ehrl P, Reuther J, Frenkel G. Al_2O_3-ceramic as material for dental implants, experimental and clinical study for the development of screw-and extension-implants. Int J Oral Surg. 1981;10(1):93–8.
37. Ali A, Singh BN, Yadav S, Ershad M, Singh SK, Mallick SP, et al. CuO assisted borate 1393B3 glass scaffold with enhanced mechanical performance and cytocompatibility: an in vitro study. J Mech Behav Biomed Mater. 2021;114:104231.
38. Moghanian A, Pazhouheshgar A, Ghorbanoghli A. Nonlinear viscoelastic modeling of synthesized silicate-based bioactive glass/polysulfone composite: theory and medical applications. Silicon. 2021;2:1–10. https://doi.org/10.1007/s12633-020-00900-9
39. Moghanian A, Nasiripour S, Hosseini S, Hosseini S, Rashvand A, Ghorbanoghli A, et al. The effect of Ag substitution on physico-chemical and biological properties of sol-gel derived 60%SiO_2-31%CaO-4%P_2O_5-5%TiO_2 (mol%) quaternary bioactive glass. Journal of Non-Crystalline Solids. 2021;560:120732. http://dx.doi.org/10.1016/j.jnoncrysol.2021.120732.
40. Li B, Liu H, Jia S. Zinc enhances bone metabolism in ovariectomized rats and exerts anabolic osteoblastic/adipocytic marrow effects ex vivo. Biol Trace Elem Res. 2015;163(1–2):202–7.
41. Jones J. Review of bioactive glass: from Hench to hybrids. Acta Biomater. 2013;9(1):4457–86.
42. Saatchi A, Arani AR, Moghanian A, Mozafari M. Cerium-doped bioactive glass-loaded chitosan/polyethylene oxide nanofiber with elevated antibacterial properties as a potential wound dressing. Ceram Int. 2021;47(7):9447–61.
43. Kazem-Rostami M, Moghanian A. Hünlich base derivatives as photoresponsive Λ-shaped hinges. Org Chem Front. 2017;4(2):224–8.
44. López-Noriega A, Arcos D, Vallet-Regí M. Functionalizing mesoporous bioglasses for long-term anti-osteoporotic drug delivery. Chem A Eur J. 2010;16(35):10879–86.
45. Moghanian A, Portillo-Lara R, Shirzaei Sani E, Konisky H, Bassir SH, Annabi N, et al. Synthesis and characterization of osteoinductive visible light-activated adhesive composites with antimicrobial properties. J Tissue Eng Regen Med. 2020;14(1):66–81. https://onlinelibrary.wiley.com/doi/abs/10.1002/term.2964

46. Song Y, Xu D, Yang R, Li D, Wu W, Guo Z, et al. Theoretical study of the effects of alloying elements on the strength and modulus of β-type bio-titanium alloys. Mater Sci Eng. 1999;260(1–2):269–74.
47. Hu S, Chang J, Liu M, Ning C. Study on antibacterial effect of 45S5 Bioglass®. J Mater Sci Mater Med. 2009;20(1):281–6.
48. Liu J, Rawlinson S, Hill R, Fortune F. Strontium-substituted bioactive glasses in vitro osteogenic and antibacterial effects. Dent Mater. 2016;32(3):412–22.
49. Enright MC, Robinson DA, Randle G, Feil E, Grundmann H, Spratt B. The evolutionary history of methicillin-resistant *Staphylococcus aureus* (MRSA). Proc Natl Acad Sci USA. 2002;99(11):7687–92.
50. Vitko NP, Richardson A. Laboratory maintenance of methicillin-resistant *Staphylococcus aureus* (MRSA). Curr Protoc Microbiol. 2013;28(1). https://doi.org/10.1002/9780471729259.mc09c02s28
51. Ben-Arfa BA, Salvado I, Ferreira J, Pullar R. The effect of functional ions (Y^{3+}, F^{-}, Ti^{4+}) on the structure, sintering and crystallization of diopside-calcium pyrophosphate bioglasses. J Non Cryst Solids. 2016;443:162–71.
52. Heidari S, Hooshmand T, Yekta B, Tarlani A, Noshiri N, Tahriri M. Effect of addition of titanium on structural, mechanical and biological properties of 45S5 glass-ceramic. Ceram Int. 2018;44(10):11682–92.
53. Rodriguez O, Stone W, Schemitsch EH, Zalzal P, Waldman S, Papini M, et al. Titanium addition influences antibacterial activity of bioactive glass coatings on metallic implants. Heliyon. 2017;3(10):e00420.
54. Asif I, Shelton R, Cooper P, Addison O, Martin R. In vitro bioactivity of titanium-doped bioglass. J Mater Sci Mater Med. 2004;25(8):1865–73.
55. Mohammadi M, Chicatun F, Stähli C, Muja N, Bureau M, Nazhat S, et al. Osteoblastic differentiation under controlled bioactive ion release by silica and titania doped sodium-free calcium phosphate-based glass. Colloids Surf B Biointerfaces. 2014;121:82–91.
56. Devi AG, Rajendran V, Rajendran N. Structure, solubility and bioactivity in TiO_2-doped phosphate-based bioglasses and glass-ceramics. Mater Chem Phys. 2010;124(1):312–8.
57. Rajendran V, Prabhu M, Suriyaprabha R. Synthesis of TiO_2-doped mesoporous nano bioactive glass particles and their cytocompatibility against osteoblast cell line. J Mater Sci. 2015;50(15):5145–56.
58. Kokubo T. Bioactive glass ceramics: properties and applications. Biomaterials. 1991;12(2):155–63.
59. Moghanian A, Firoozi S, Tahriri M. Synthesis and in vitro studies of sol-gel derived lithium substituted 58S bioactive glass. Ceram Int. 2017;43(15):12835–43.
60. Yellowley C, Li Z, Zhou Z, Jacobs CR, Donahue H. Functional gap junctions between osteocytic and osteoblastic cells. J Bone Miner Res. 2000;15(2):209–17.
61. Moghanian A, Zohourfazeli M, Tajer M. The effect of zirconium content on in vitro bioactivity, biological behavior and antibacterial activity of sol-gel derived 58S bioactive glass. J Non Cryst Solids. 2020;546:120262. https://www.sciencedirect.com/science/article/abs/pii/S0022309320303756
62. Hu S, Ning C, Zhou Y, Chen L, Lin K, Chang J. Antibacterial activity of silicate bioceramics. J Wuhan Univ Technol Mater Sci Ed. 2011;26(2):226–30.
63. Hajifathali Z, Moghan A. The effect of substitution of CaO/MgO and CaO/SrO on in vitro bioactivity of sol-gel derived bioactive glass. Int J Biomed Biol Eng. 2019;13(6):279–87.
64. Moghanian A, Sedghi A, Ghorbanoghli A, Salari E. The effect of magnesium content on in vitro bioactivity, biological behavior and antibacterial activity of sol-gel derived 58S bioactive glass. Ceram Int. 2018;44(8):9422–32.
65. Zhong Z, Qin J, Ma J. Electrophoretic deposition of biomimetic zinc substituted hydroxyapatite coatings with chitosan and carbon nanotubes on titanium. Ceram Int. 2015;41(7):8878–84.
66. Bargavi P, Chitra S, Durgalakshmi D, Rajashree P, Balakumar S. Effect of titania concentration in bioglass/TiO_2 nanostructures and its in vitro biological property assessment. J Nanosci Nanotechnol. 2018;18(7):4746–54.
67. Danewalia S, Singh K. Intriguing role of TiO_2 in glass-ceramics: bioactive and magneto-structural properties. J Am Ceram Soc. 2018;101(7):2819–30.
68. Martin RA, Moss R, Lakhkar N, Knowles J, Cuello G, Smith M, et al. Structural characterization of titanium-doped bioglass using isotopic substitution neutron diffraction. Phys Chem Chem Phys. 2012;14(45):15807–15.
69. Beherei H, Mohamed K, El-Bassyouni G. Fabrication and characterization of bioactive glass (45S5)/titania biocomposites. Ceram Int. 2009;35(5):1991–7.
70. Miyata N, Fuke K-I, Chen Q, Kawashita M, Kokubo T, Nakamura T. Apatite-forming ability and mechanical properties of PTMO-modified CaO–SiO_2–TiO_2 hybrids derived from sol-gel processing. Biomaterials. 2004;25(1):1–7.
71. ElBatal H, Azooz M, Khalil E, Monem A, Hamdy Y. Characterization of some bioglass–ceramics. Mater Chem Phys. 2003;80(3):599–609.
72. Moghanian A, Firoozi S, Tahriri M, Sedghi A. A comparative study on the in vitro formation of hydroxyapatite, cytotoxicity and antibacterial activity of 58S bioactive glass substituted by Li and Sr. Mater Sci Eng. 2018;91:349–60.
73. Elsa M, Moghanian A. Comparative study of calcium content on in vitro biological and antibacterial properties of silicon-based bioglass. Int J Chem Mol Eng. 2019;13:288–95. https://publications.waset.org/10010511/comparative-study-of-calcium-content-on-in-vitro-biological-and-antibacterial-properties-of-silicon-based-bioglass
74. Stoch A, Jastrzębski W, Brożek A, Trybalska B, Cichocińska M, Szarawara E. FTIR monitoring of the growth of the carbonate containing apatite layers from simulated and natural body fluids. J Mol Struct. 1999;511:287–94.
75. Abou Neel E, Knowles J. Physical and biocompatibility studies of novel titanium dioxide doped phosphate-based glasses for bone tissue engineering applications. J Mater Sci Mater Med. 2008;19(1):377–86.
76. Moghanian A, Ghorbanoghli A, Kazem-Rostami M, Pazhouheshgar A, Salari E, Saghafi Yazdi M, et al. Novel antibacterial Cu/Mg-substituted 58S-bioglass: synthesis, characterization and investigation of in vitro bioactivity. Int J Appl Glass Sci. 2019;11:604–18. https://ceramics.onlinelibrary.wiley.com/doi/abs/10.1111/ijag.14510
77. Khvostenko D, Hilton T, Ferracane J, Mitchell J, Kruzic J. Bioactive glass fillers reduce bacterial penetration into marginal gaps for composite restorations. Dent Mater. 2016;32(1):73–81.

How to cite this article: Moghanian A, Nasiripour S, Koohfar A, et al. Characterization, in vitro bioactivity and biological studies of sol-gel-derived TiO_2 substituted 58S bioactive glass. *Int J Appl Ceram Technol*. 2021;00:1–12. https://doi.org/10.1111/ijac.13782